EMC Absorbers and Indoor EMC Test Chambers

KEFENG LIU
EMC Test Systems, Austin, TX*

The fundamental properties of RF absorbers must be understood when building indoor shielded testing facilities.

INTRODUCTION

Indoor shielded EMC test sites have become more and more popular during the past two decades. The obvious advantages of the indoor shielded test site over Open Area Test Sites (OATS) are its inherent site efficiency and its immunity to ambient noise and weather conditions. Since the chamber simulates the OATS test environment in a shielded enclosure, reflections from the walls of the shielded enclosure must be effectively suppressed. Moreover, Federal Communications Commission (FCC) and European Standards require that the radiated emissions of unintentional sources are to be measured from as low as 30 MHz, so shielded EMC chambers must also provide acceptable measurement accuracy at the same frequency range. The International Electrotechnical Commission (IEC) also defines the uniform field requirements for conducting radiated immunity tests of electronic devices from as low as 26 MHz to as high as a few GHz.

Frequently, it is a more challenging problem for a shielded EMC chamber to meet the site requirements on radiated emission testing at the low end of the frequency range (i.e., 30 MHz to 150 MHz). The crux of the problem is the performance of RF absorbers on the metallic surface at the low frequency range. An EMC test engineer who wants to build a shielded EMC chamber must understand the properties of the RF absorber and the design criteria to achieve the requirements. This article discusses existing RF absorber properties and EMC chamber designs.

EMC ABSORBERS

RF absorbers for EMC applications in shielded semi-anechoic chambers can be classified into three types: electrical (dielectric) absorbers, magnetic absorbers (ferrite tiles), and hybrid absorbers (combinations of ferrite tile and foam absorbers).

DIELECTRIC ABSORBERS

Dielectric absorbers are typically made of carbon-loaded polyurethane foam constructed in pyramidal shapes. The electromagnetic wave absorbing properties of these absorbers is derived from the lossy part of complex permittivity (ε_r) resulting from the carbon loading of the polyurethane foam. The dielectric absorber interacts with the electric field for RF energy absorption.

To maximize the absorbing material efficiency, a good portion of dielectric absorbing media should be located in the region where the electric field is maximized. With a metallic backing surface, the tangential electric field is nullified on the metallic surface, and maximized at a quarter wavelength away from the metallic surfaces. Due to this fundamental limitation, dielectric absorbers for EMC applications are always designed with length in the proximity of at least a quarter of the wavelength at its lowest operating frequency.[1] Therefore, 8′ long dielectric absorbers are most commonly used for EMC chambers which operate as low as 30 MHz.

In addition to the absorber length requirement, the lossy material loading of the foam and the shape of the pyramidal construction also contribute to the performance of dielectric absorbers. In the past, flat top and/or hollow pyramid designs have been investigated.[1] In addition, a twisted pyramidal shape was also introduced to construct the absorber element. While twisted pyramids are mechanically robust for installing absorbers for EMC applications, their absorbing performance is inferior to pyramidal absorbers constructed to the same length.

MAGNETIC ABSORBERS

Magnetic absorbers primarily interact with the magnetic field for RF energy absorption. Therefore, they fully utilize the advantage of the metallic surface on the shielded wall since the magnetic field is maximized on the metallic surface. By installing magnetic absorbers on the shielded wall, the absorbing properties of the magnetic absorber will be enhanced and can reach maximum capability. With proper design, magnetic absorbers have a very good normal incident absorbing property at as low as 30 MHz and as thin as a few millimeters in height compared to dielectric absorbers of about 2.4 meters or more for the same performance.

Three different types of magnetic absorbers are commercially available: flat ferrite tile, grid ferrite tile, and silicon rubber-based sheets. Both flat and grid ferrite tiles are soft ferrite materials. The key ingredients of soft ferrite are the nickel-zinc-ferromagnetic compounds. The low-frequency absorption of the soft ferrite loss is obtained by using ceramic technology for both high permeability and high loss tangent, key parameters to the performance of the ferrite tile absorber. With proper design, both flat and grid ferrite tiles can achieve reasonable absorbing performance between 30 and 1000 MHz. However, due to their high

*See advertisement on back cover.

permeability, the absorbing property of both ferrite tiles is very sensitive to the air gaps between tiles.[2,3,4]

Silicon rubber-based sheet absorbers normally do not have permeability and loss tangent as high as those of ferrite tile. They are fabricated as weatherproof narrowband microwave absorbers. They are also incorporated with ferrite tiles to act as a tuning element to extend performance at higher frequencies.

Magnetic absorbers are usually fabricated into thin flat layers and tuned to a defined frequency band. Normally, they have a much higher gravity density compared to the dielectric absorbers. However, they are much more compact in absorber length than dielectric absorbers and are especially effective at low frequencies.

HYBRID ABSORBERS

Hybrid absorbers are combinations of ferrite tile and dielectric absorbers (Figure 1). They are designed to combine the advantages of both dielectric and ferrite tile absorbers. The ideal hybrid absorber performance relay allows ferrite tile to absorb the incident RF energy at low frequencies (between 30 and 100 MHz) and allows the dielectric absorber to take over the absorption above 100 MHz (up to 40 GHz). In reality, since the magnetic and dielectric absorbers are too dissimilar in wave impedance, such a relay of absorbing performance is very difficult to design. If the complex permittivity of the dielectric absorber is not designed properly, it is possible that a catastrophic loss of performance of both types of absorber may occur at low frequency. To avoid this cancellation of performance, it is necessary to have a very low lossy loading of the foam absorber. This condition makes the hybrid absorber design very delicate at the frequency range of 30 to 120 MHz.

The ferrite tile and hybrid absorbers are becoming more and more popular due to their compact physical sizes. When designed properly, they can be very effective EMC absorbers, well-suited for indoor shielded EMC chambers (Figures 2 and 3).

In many cases, the performance of ferrite tiles (flat or grid tiles) is determined by measuring the return loss of small toroid samples in a circular coaxial air line. Since there is no discontinuity along the magnetic line inside the circular coaxial airline, the air gap effects on the absorbing performance of the ferrite tile absorbers (including the hybrid absorbers) are not measured. In an EMC chamber, however, the absorbing property is provided by the wall, which consists of many air gaps between the ferrite tiles. Therefore, the installed wall absorber performance will be substantially different from those intrinsic properties. This article presents a few simplified formulas to analyze the absorbing properties of the ferrite tile absorber and to quantify the effects of air gaps.

ANALYSIS

Figure 4 shows a typical geometry of the ferrite tile absorber mounted on the metallic surface. The reflection coefficient can be expressed by

$$\Gamma = \frac{E_r}{E_i} = \frac{\eta_t - \eta_o}{\eta_t + \eta_o} \qquad (1)$$

where

Γ = reflection coefficient

η_o = free-space wave impedance

h_t = wave impedance of the ferrite tile mounted on the metallic surface, which can be expressed as

$$\eta_t = \eta_o \sqrt{\frac{\mu_r}{\varepsilon_r}} \tanh\left(\frac{2\pi t}{\lambda_o}\sqrt{\mu_r \varepsilon_r}\right) \qquad (1a)$$

where

μ_r = complex relative permeability

ε_r = permittivity

t = thickness of the ferrite tile

λ_o = free-space wavelength

Therefore, at about 30 MHz, since the thickness of the tile is much smaller than the wavelength,

$$\tanh\left(\frac{2\pi t}{\lambda_o}\sqrt{\mu_r \varepsilon_r}\right) \rightarrow j\frac{2\pi t}{\lambda_o}\sqrt{\mu_r \varepsilon_r} \qquad (1b)$$

Thus, the wave impedance of the ferrite tile wall can be expressed as

$$\eta_t \approx j\eta_o \mu_r \frac{2\pi t}{\lambda_o} \qquad (1c)$$

In Equation (1c), one can notice that the wave impedance of the ferrite tile is independent of the complex permittivity at low frequency where (1b) is valid. Substituting (1c) into (1), and using $\mu_r = \mu'_r - j\mu''_r$, Equation (1) can be further expressed as

$$\Gamma = \frac{\left(\frac{2\pi t}{\lambda_o}\mu''_r - 1\right) + j\frac{2\pi t}{\lambda_o}\mu'_r}{\left(\frac{2\pi t}{\lambda_o}\mu''_r + 1\right) + j\frac{2\pi t}{\lambda_o}\mu'_r} \qquad (2)$$

Since the thickness of the tile is designed so that at the tuning frequency near the low end (i.e., 30

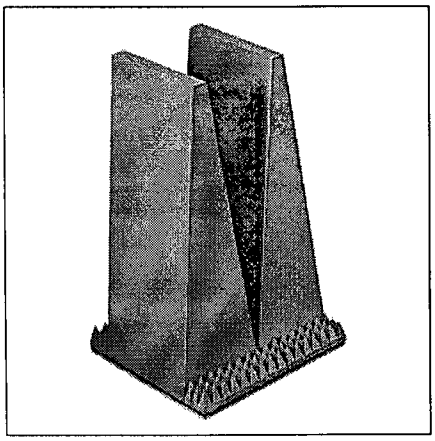

***Figure 1**. Hybrid Absorber.*

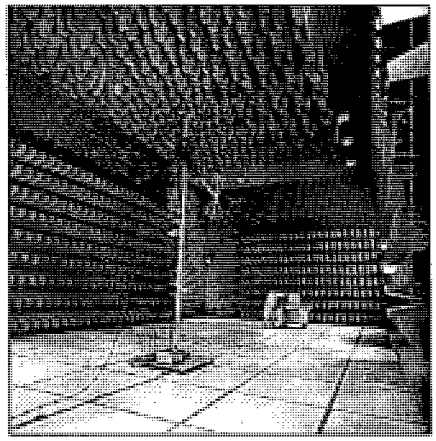

***Figure 2**. 10-Meter Chamber with Antenna Tower and EUT.*

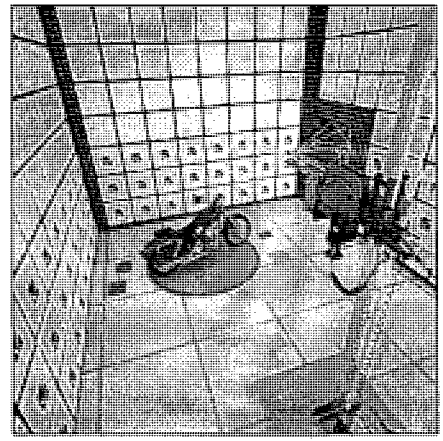

***Figure 3**. 3-Meter Chamber with Antenna Tower and EUT.*

MHz), $\frac{2\pi t}{\lambda_0}\mu''\to 1$, it can be shown that the reflectivity can be empirically expressed as

$$R = 20\log_{10}(\Gamma) \approx -20\log_{10}(\frac{2\mu_r''}{\mu_r'}) \qquad (3)$$

Equation (3) describes a very simple relationship between the normal incident reflectivity performance of the ferrite tile absorber and the loss tangent of the intrinsic permeability. It also helps to find ways to improve the performance of the ferrite tile absorber by increasing the loss tangent of the intrinsic permeability. Figure 5 shows the complex permeability of one of the commercial ferrite tile absorbers. The permittivity of the compound is approximately equal to 11. Figure 6 shows the comparison of reflectivity performances using Equations (1) and (3). As demonstrated, Equation (3) provides very good approximation below 50 MHz and remains valid up to about 100 MHz. Above 100 MHz, the complex permittivity of the ferrite tile starts to impact the validity of Equation (1b). If ε_r can be kept close to unity, the validity of Equation (3) can be further extended.

AIR GAP EFFECTS

Since the permeability of the ferrite tiles is much larger than unity, the effect of air gaps between ferrite tile on the absorbing performance can be very serious. Such an impact is analogous to the effect of air gap in the soft iron core of the AC power transformer.

To provide a quantified analysis, the transformer core air gap formula based on magnetic circuitry theory is introduced to calculate the effective permeability of the tile wall with air gaps:

$$\mu_r^e = \frac{\mu_r}{1 + \frac{\Delta}{\ell}(\mu_r - \mu_{air})} \qquad (4)$$

where

Δ = the dimension of air gap perpendicular to the magnetic field line

ℓ = the width of the ferrite tile

Equation (4) has been compared to more rigorous methods such as the Finite Element Method, and was found to be in excellent agreement as long as the air gap is comparatively small to the tile dimensions.

In Figure 7, the width of the ferrite tile is 100 mm and the thickness is assumed to be 6.35 mm. As shown, the return loss at normal incidence suffers a very severe degradation due to the existence of air gaps from 30 MHz to 200 MHz. An air gap which averages 0.2 mm (i.e., the thickness of a piece of paper) can degrade the intrinsic -18.5 dB return loss to worse than -10 dB at 30 MHz. Such an air gap effect has also been confirmed by data measured in a 1.84 m x 1.84 m coax reflectometer and by Reference 2.

GRID TILES

The performance of grid tiles was also analyzed. The performance of grid ferrite tile walls was found to be less sensitive to air gaps compared to that of flat tile walls. Figure 8 shows an analysis of 19-mm thick commercial grid tiles. The analysis shows that the grid tile can retain a -15 dB normal incident reflectivity performance compared to a marginal -10 dB from a flat ferrite tile for an assumed 0.2 mm average air gap between tiles. It was also found that the grid

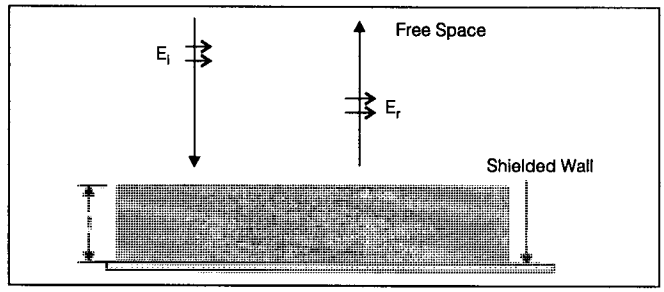

***Figure 4**. Ferrite Tile Mounted on the Metallic Surface.*

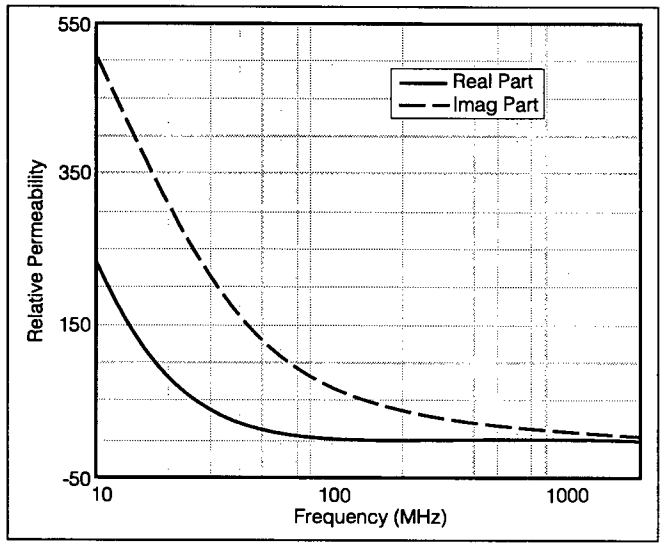

***Figure 5**. Typical Relative Permeability of Ferrite Tile.*

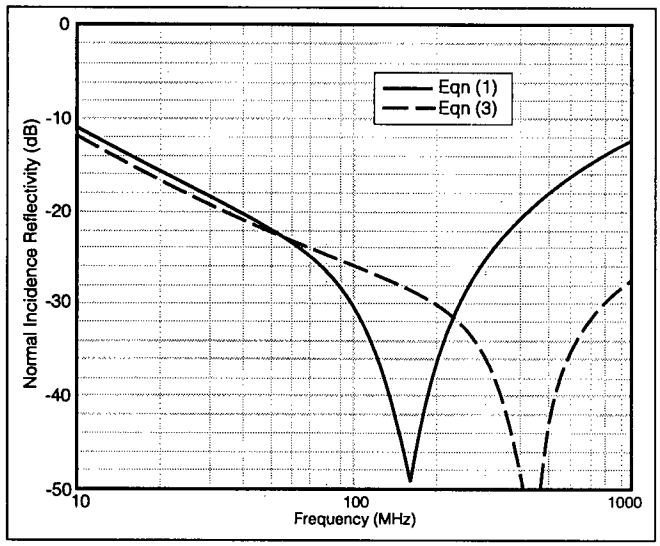

***Figure 6**. Comparison of Equations (1) and (3).*

tile has about 50% of the ferrite material active per polarization. Therefore, the grid tile requires twice the volume of sintered ferrite material as that of flat tile. Due to its grid shape, the effective permeability and permittivity is reduced to less than one third of the bulk material values. This reduced permeability is compensated for by the increased thickness to maintain tuning condition at low frequencies. Due to its reduced permeability, the degradation of performance from air gaps is significantly less than that of the flat tile. Owing to its reduced effective permittivity, the performance is extended to higher frequencies. The two added advantages of absorbing performance is gained at the cost of the increased volume of sintered ferrite material.

HYBRID ABSORBERS

It becomes apparent that the air gap severely impacts the performance of hybrid absorbers. Without accounting for air gap impact, the design absorber performance does not correspond to the installed wall performance in an EMC chamber. Such a difference is easily observable in an EMC chamber built for 10-m test range testing. The air gap degradation of absorber and chamber performance is very pronounced between 30 and 100 MHz. However, if the gap condition is more severe, EMC chamber performance problems can also be measured above 100 MHz. In order to minimize air gap degradation of the ferrite tiles, the matching foam absorber has to be deep enough to alter the wave impedance before entering the ferrite tile wall so that ferrite tile can still absorb the most significant portion of RF energy from the incident wave at about 30 MHz. For example, hybrid absorbers for a 10-m EMC chamber would normally require at least 1 m in total absorber height. Such a height and the shape of the absorber element are necessary to maintain the transition from low wave impedance region (dielectric absorber region) to high impedance region (magnetic absorber region).

Figure 9 illustrates the design and measured performances of a hybrid absorber. It was designed with measured complex reflection coefficients from ferrite tile panels installed in a coax waveguide reflectometer, with dimensions of 17 m in length and 1.84 m x 1.84 m in square cross section.

Figure 10 presents the comparison of design and measured performance for an improved 1-m hybrid absorber design with a different ferrite tile thickness and a shorter foam absorber. A significant enhancement of absorbing performance between 50 and 120 MHz is shown.

The hybrid absorber has been installed in two 10-m EMC chambers and successfully meets the FCC site certification testing requirements.

While the absorber performance at normal incidence has been the usual design and measured parameter for most RF absorbers, it is also necessary to point out that the oblique incident angle performance of the absorber is an equally or even more important parameter for EMC chamber design.

As shown in Figure 11, the return loss performance of the RF absorber degrades as the angle of incidence increases.

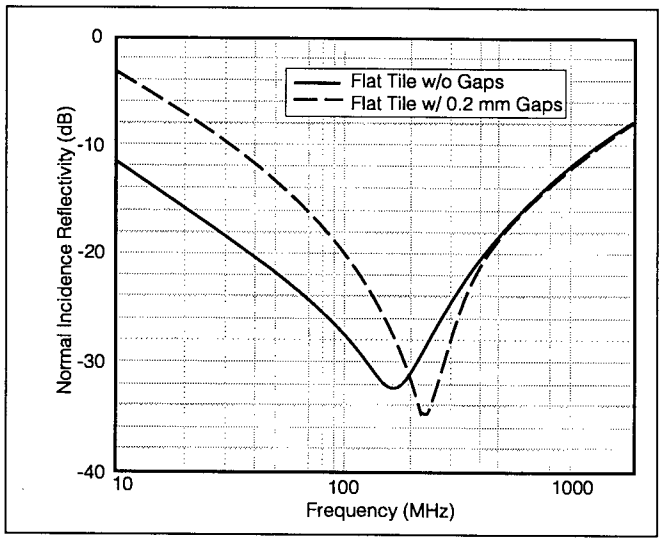

***Figure 7**. Flat Tile Air Gap Degradation.*

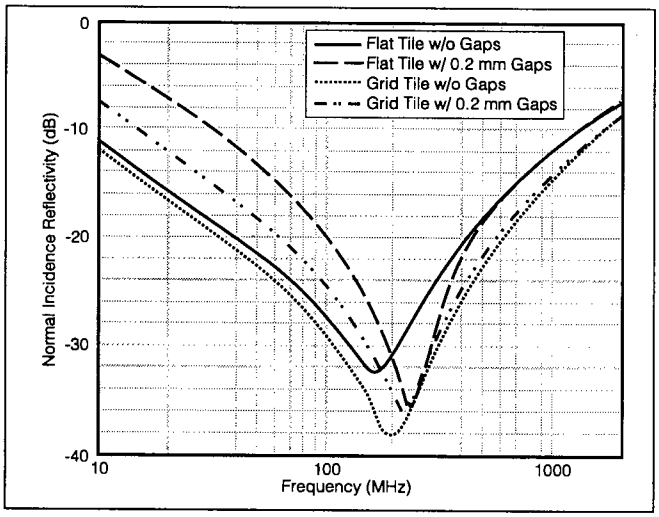

***Figure 8**. Comparison of Air Gap Degradation Between Flat and Grid Ferrite Tiles.*

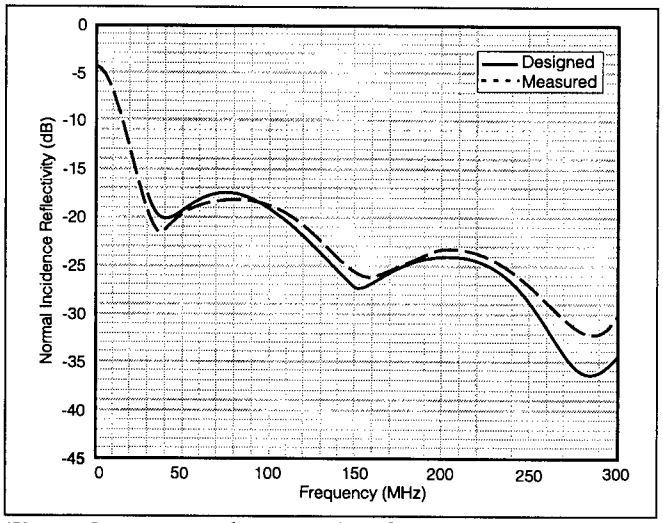

***Figure 9**. Design and Measured Performance of a Hybrid Absorber.*

For incidence angles of greater than 60°, the absorber becomes very ineffective at low frequencies. Typically, one needs to design the chamber dimensions so that incident angles on the chamber walls are less than 45°. This is the fundamental limiting factor which prevents one from building super compact EMC chambers.

The measurement of oblique incident angle absorber performance at low frequencies (30 to 100 MHz) has not been reported. One fundamental difficulty is obtaining the sample dimensions that are required to make sensible measurement become logistically impractical. One typical practice is to use the measured normal incident performance to calibrate the accuracy of the numerical calculation. If the normal incidence reflection coefficient is predicted accurately, the oblique incident performance should be reasonably accurate using the same numerical model. Such a practice has been proven to be very effective in predicting the chamber performance.

EMC CHAMBER DESIGN

Having fully characterized the EMC absorbers, computer models can also be introduced to predict the chamber performance. A computer program based on the multiple-order ray-tracing technique published in Reference 5 has been developed to simulate the chamber NSA performance. The PC-based software has been extensively analyzed and correlated to actual chamber constructions to study the validity of the method.

Figure 12 shows predicted NSA performance of a 10-m EMC chambers in which a hybrid absorber was installed. The Normalized Site Attenuation (NSA) performance is shown for vertical polarization since it is usually more difficult to comply with site certification requirements for vertical polarization than for horizontal polarization. The five NSA curves correspond to the predicted NSA performance of the EMC chamber at the center of the 4 m-diameter turntable, and four other positions that are 2 m from the center of the turntable. The transmit antenna is positioned at 1 m above the ground plane, while the receive antenna scans between 1 and 4 m in height.

Figure 13 presents measured NSAs at the corresponding positions. As shown in both Figures 12 and 13, an excellent comparison between predicted and measured NSA performance is demonstrated for the 10-m test range.

Through extensive modeling, the first-order reflection model is found to be inadequate to predict meaningful NSA performance of an EMC chamber. The predicted result is typically pessimistic for horizontal polarization, while the result for vertical polarization is grossly optimistic. In order to predict the NSA performance accurately, it is necessary to incorporate up to 4 bounces for sidewalls and end walls, and 9 bounces for floor and ceiling reflections. Further increases of reflection orders do not result in any observable improvement in predicted NSA performance for an EMC chamber installed with good absorbers.

Also, the predicted NSA data for a compactly sized chamber built for the 3-m test distance does not correlate to the measured data as accurately as the larger chamber built for the 10-m test distance. Further investigations are underway to improve this deficiency.

Although more rigorous numerical packages are also available to simulate the performance of the chamber, the ray-tracing technique is still the preferred method because of its efficiency. Moreover, the accuracy achieved using the ray-tracing technique should be within the product/installation variations.

SUMMARY

Physical properties of dielectric and ferrite related absorbers have been discussed. A few empirical formulas for ferrite tile performance were presented for quick evaluation of intrinsic ferrite tile performance at low frequencies. A simplified formula for modeling the air gap effect of ferrite tile has been validated for an effective evaluation of EMC absorber walls with ferrite tile. Finally, fully characterized hybrid ab-

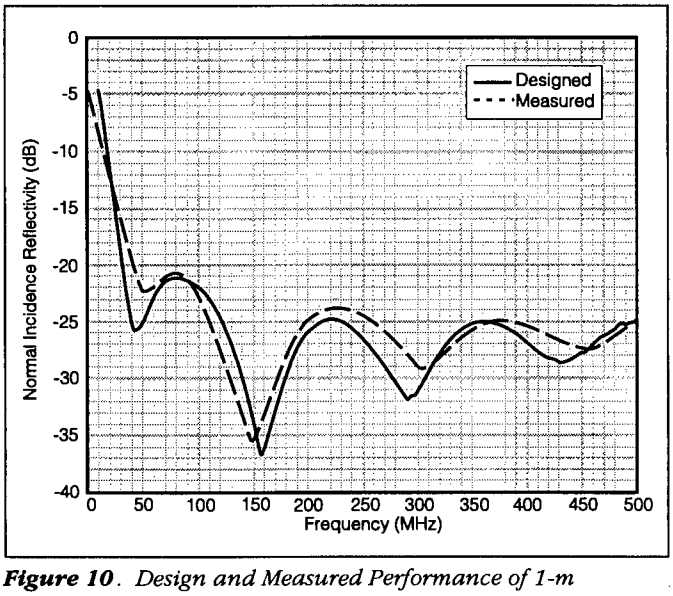

***Figure 10**. Design and Measured Performance of 1-m Hybrid Absorber.*

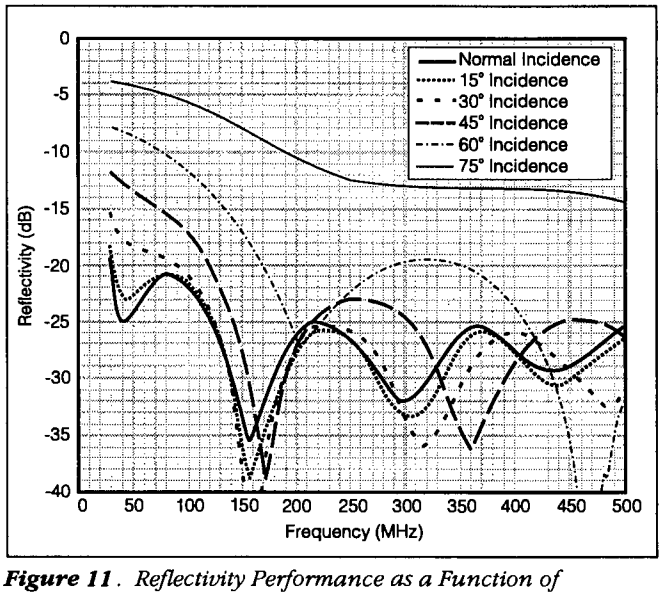

***Figure 11**. Reflectivity Performance as a Function of Incidence Angle for 1-meter Absorber.*

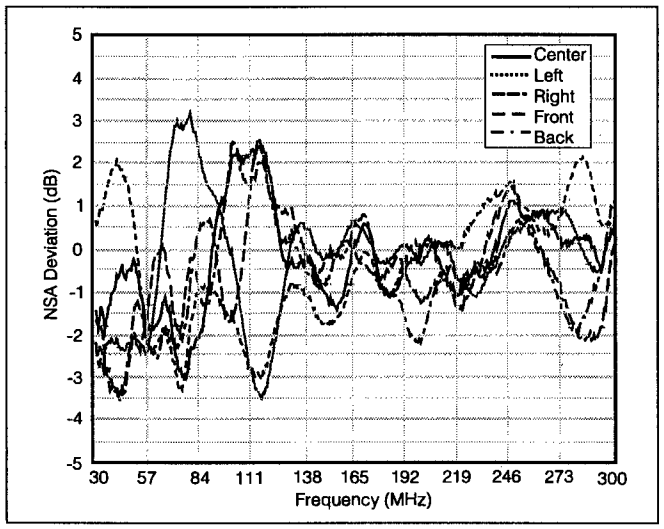

***Figure 12**. Predicted NSA Deviation from Theoretical NSA in an EMC Chamber at 10-m Test Distance.*

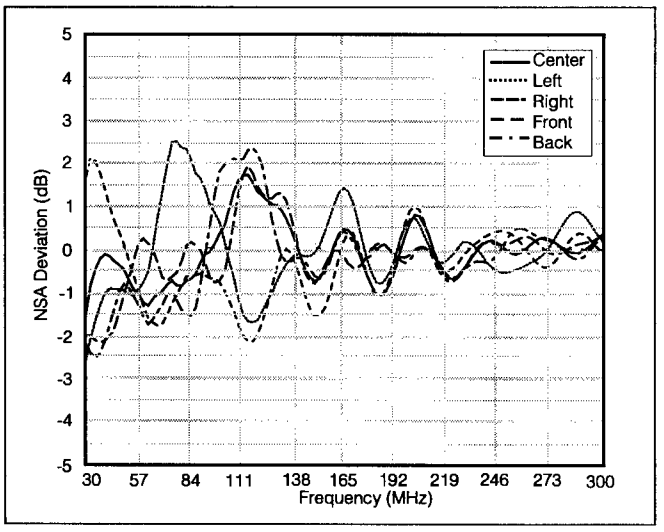

***Figure 13**. Measured NSA Deviation from Theoretical NSA in an EMC Chamber at 10-m Test Distance.*

sorber reflection coefficients were used to predict the performance of the EMC chamber and were shown to correlate to the measured data very well at the 10-m test range.

Recent RF absorber developments, especially the use of ferrite absorbers, have made indoor shielded EMC test facilities more and more cost-effective and feasible to EMC test site users. The use of computational techniques has made the design of EMC chambers predictable to very good accuracy levels. With the use of a floor absorber treatment, the same shielded EMC chamber can be converted to perform radiated immunity testing of the same electronic device.

REFERENCES

1. K. Liu, and J. M. Kilpela, "Optimized Absorber Designs for EMC Applications," *Proceedings of The 1993 IEEE International Symposium on EMC*, Dallas, TX, August 9-13, 1993, pp. 289-292.
2. S. Takeya, and K. Shimada, "New Measurement of RF Absorber Characteristics by Large Coaxial Line," *Proceedings of The 1993 IEEE International Symposium on EMC*, Dallas, TX, August 9-13, 1993, pp. 397-402.
3. H. Anzai, Y. Naito, and T, Mizumoto, "Effect of Ferrite Tiles' Gap on Ferrite Electromagnetic Wave Absorber," *Proceedings of The 1995 IEEE International Symposium on EMC*, Atlanta, GA, August 14-18, 1995, pp. 297-302.
4. K. Liu,, "Analysis of the Effect of Ferrite Tile Gap on EMC Chamber Having Ferrite Absorber Walls Optimized Absorber Designs for EMC Applications," *Proceedings of The 1996 IEEE International Symposium on EMC*, Seattle, WA, August 19-23, 1996, pp. 156-161.
5. J. D. Gavenda, "Semi-anechoic Chamber Site Attenuation Calculations," *Proceedings of The 1990 International Conference on Electromagnetic Compatibility*, York, UK, August 28-31, 1990, pp. 109-113.
6. H. F. Pues, "Electromagnetic Absorber Measurement in a Large Waveguide," *Proceedings of The 8th International Zürich Symposium and Technical Exhibition on Electromagnetic Compatibility*, Zürich, Switzerland, March 1989, pp. 253-258.

***KEFENG LIU** is the Senior Principal Engineer at EMC Test Systems, Austin, TX. His research interests and industrial expertise include numerical simulation of electromagnetic radiation and scattering using integral equation and moment methods; frequency and time domain measurement of antenna radiation and radar cross-section in an anechoic chamber; measurement of electromagnetic properties of materials using network analyzers; analysis and design of RF absorbers and anechoic chambers for antenna/RCS and EMC applications. He is a member of the IEEE APS, MTT and EMC Societies. He is also the author or co-author of 20 papers published in professional journals. (512) 835-4684.*